

Modification of high-density polyethylene using functionalized titanium dioxide nanoparticles

Aline Souza Salum^{1,3}, Paulo Apolinário da Silva Veiga¹,
Tarcisio Loddi², Joseane Valente Gulmine³, Vitoldo Swinka Filho^{1,3}

¹Universidade Federal do Paraná (PIPE/UFPR), Av. Cel. Francisco H. dos Santos, 100 - Jardim das Américas, CEP: 81531-980, Curitiba, Paraná, Brazil

²Companhia Paranaense de Energia (COPEL), R. Antônio Krasinski, 141 - Orleans, CEP: 81200-410, Curitiba, Paraná, Brazil

³Instituto de Tecnologia para o Desenvolvimento (Lactec), Rodovia BR-116, Km 98, 8813, Jardim das Américas, CEP: 81531-980, Curitiba, Paraná, Brazil

E-mail addresses: alinesalum@gmail.com; jogulmine@yahoo.com.br; vitoldo@lactec.org.br

ABSTRACT

High-density polyethylene (HDPE) has many applications, including in the electrical sector, due to its excellent electrical, mechanical, and thermal properties. In insulators employed in electricity networks, the material is exposed to various adverse conditions (solar radiation, humidity, temperature cycles, and pollution), which can accelerate degradation of the polymer, modifying its properties and affecting its performance in the field. The surface resistivity of HDPE hinders the transmission of electrical current on the surface, consequently avoiding tracking. However, factors such as contamination of the surface by industrial pollutants, salt, and other agents, together with high humidity, act to decrease the surface resistivity, facilitating the flow of current between different potentials and initiating the electrical tracking process, which can lead to loss of the insulation property. In order to avoid electrical tracking, it is important to prevent the adhesion of dirt on the surface of the insulator, which can be achieved by the provision of a hydrophobic surface. The aim of this work was to modify the surface of HDPE using a coating of TiO₂ nanoparticles. The nanoparticles were functionalized to optimize adhesion to the polymer surface during immersion processes, obtaining hydrophobic surfaces with self-cleaning characteristics that could improve performance when applied to insulators. Four different functionalization agents were studied, with different carbon chain lengths: trimethoxypropylsilane (TMPSi), trimethoxyoctylsilane (TMOSi), trimethoxyhexadecylsilane (TM16Si), and trimethoxyoctadecylsilane (TM18Si). The modification of the nanoparticle surface was confirmed by analysis using Fourier transform infrared (FTIR) spectroscopy. The HDPE sample surfaces showed good adhesion of the functionalized nanoparticles, with enhanced hydrophobicity.

Keywords: High-density polyethylene; hydrophobicity; surface modification; functionalized TiO₂; silanes.

1. INTRODUCTION

High-density polyethylene (HDPE) is a semi-crystalline, flexible, inert, non-polar thermoplastic polymer, which presents crystallinity above 90%, and low levels of branching. Its crystallinity melting temperature is approximately 132°C, density between 0.95 and 0.97 g/cm³, and average numerical weight in the range of 50,000 to 250,000. The linearity of the chains makes the orientation, alignment and packing of the long chains, as well as intermolecular curtains (Van der Waals) act with greater intensity, and as a consequence, the crystallinity and melting temperature also increase. The orientation of polymer chains also has a strong effect on the mechanical properties of the polymer [1, 2].

In general, HDPE is quite inert and has low chemical reactivity. The most reactive regions of molecules are as double end bonds and as tertiary CH bonds in branches. It is stable in alkaline solutions of any concentration and in saline solutions, regardless of pH, it also does not react with organic acids, HCl or HF; concentrated solutions of H₂SO₄ (> 70%) at high temperatures react slowly with HDPE, producing sulphoderivatives. At room temperature, HDPE is not soluble in any known solvents, although many solvents, such as xylene, for example, have a swelling effect. At high temperatures, HDPE dissolves in some aliphatic

and aromatic hydrocarbons [1]. HDPE is used in different segments of the industry and can be molded by different thermoplastic manufacturing processes.

Titanium dioxide, TiO₂, found in nature in natural or synthesized minerals, has three allotropic phases: anatase, rutile and brookite [3]. The anatase and rutile phases have a tetragonal structure and the brookite phase, orthorhombic. The anatase and brookite phases are metastable, which exothermically and irreversibly transform into rutile [4]. The anatase-rutile phase transformation does not have a defined transition temperature, as there is no phase equilibrium, so the transformations can occur over a wide temperature range, ranging from 350 to 1175 °C, as it is influenced by the method of sample preparation, the presence of impurities or additives and by the atmosphere present during the process. The brookite phase is difficult to be synthesized, thus, commercially the anatase and rutile phases are produced [3, 4].

The main application of titanium dioxide is as a white pigment in paints, food colors, cosmetics, toothpastes, polymers and other cases where white coloring is desired [3, 4]. This is due to the high refractive indices of rutile and anatase, which result in high surface reflectivity. Consequently, small particle size and large surface areas are used due to the resulting opacity power and gloss [3]. The rutile phase is favorable for self-cleaning and superhydrophobic surfaces [5].

Nanomaterials based on titanium dioxide (TiO₂) have attracted considerable interest in the engineering area, due to their many applications, such as in solar cells, fuel cells, chemical sensors, paints, pigments, photodegradation of pollutants, and self-cleaning surfaces [6-10]. Due to their small solid-liquid contact area and large specific surface area, TiO₂ nanoparticles have been used to produce hydrophobic and superhydrophobic surfaces [6, 7, 11-13].

On a molecular scale, surfaces can be classified as polar or nonpolar, depending on their chemical composition. There have been many studies of the wettability of surfaces with different chemical characteristics, with polar surfaces tending to be hydrophilic, while most nonpolar surfaces are hydrophobic. In addition to the effects of polarity, the topography of the surface (such as roughness) is another important factor affecting wettability. It has been found that polar materials with atomic scale roughness can present hydrophobic characteristics [14]. The methods most widely used for surface modification involve depositing thin layers of chemically modified (functionalized) particles or nanoparticles, or the application of coatings [6, 7, 11, 15-17]. The application techniques employed include sol-gel, vapor deposition, and electrochemical methods, among others [6].

The use of titanium dioxide (TiO₂) nanoparticles to modify the surface of HDPE can increase the hydrophobicity and confer self-cleaning properties. Meanwhile, most of the polymeric resins and composites employed industrially have low free surface energy and lack surface polar functional groups, resulting in poor adhesion of these particles [18].

Nanoparticles (NPs) have weak interactions with polymer surfaces, due to their polarity and chemical nature, so it is necessary to functionalize their surfaces with compounds possessing chemical species that have greater affinity for the polymeric matrices. These species are usually organic chains that act to increase the interaction and consequently improve adhesion between the particles and the surface [19]. The use of functionalization enables the addition of specific molecules or functional groups to the surface of the nanoparticle, altering its properties. As a simplification, the functionalized nanoparticle consists of a central nucleus and a surface with organic molecules attached around it.

Electric energy has become indispensable to human society. In order to arrive at the consumer, the energy passes through a complex system of generation, transmission, and distribution. The generation of electricity occurs in thermal, hydraulic, nuclear, wind, and solar plants, among others. In the transmission stage, the energy is transported through transmission networks to distribution substations and large-scale consumers. In the distribution stage, the energy is transported from the substations to the final consumer. The systems consist of metal towers, posts, and suspended cables that are either bare or coated with polymeric material, in addition to insulators [20].

Interruptions of the electricity supply occur due to failures in the system, with one of the main causes being related to electrical insulators whose function is to safely separate parts with high electrical potential from those with lower potential, such as the electrified lines of posts and towers. The insulators are produced from dielectric materials including glass, porcelain, and polymers. Dielectric materials possess insulator characteristics, up to a certain electric field limit. When the limit is exceeded, the material begins conducting current and its dielectric strength has been exceeded [21].

Polymeric insulators have progressively replaced those composed of glass and porcelain since they offer advantages including lower manufacturing cost, lighter weight, easier transport, and greater resistance to vandalism. Their main disadvantage lies in the difficulty in detecting signs of deterioration, which is most

easily observed when the components are about to fail, consequently hindering preventive maintenance and their replacement [21, 22]. High-density polyethylene (HDPE) is an attractive material for use in the electricity sector and has already been employed in various polymeric components of electric energy distribution networks, in accordance with Brazilian technical standards [23-26].

Polymeric materials exposed to the external environment are liable to degradation due to the effects of factors such as solar radiation, humidity, cycles of temperature, and pollution. It has been shown that UV radiation, associated with the effects of humidity, temperature, and pollutants, can accelerate degradation processes. However, there is no consensus in the scientific community regarding the factors that have the greatest influence on the aging process [27-31].

In addition to environmental conditions, factors related to the synthesis and processing of the polymeric material can influence its degradation rate, including the presence of unsaturation (due to the polymerization) [32] and metal ions (from processing and manufacture). Degradation processes may be accelerated by mechanical stresses arising in the material, associated with aging [33] and the exposure to contamination that can occur due to the presence of agrochemicals in agricultural regions [34], proximity to industries, or installation in coastal regions.

As already mentioned, one of the factors that can cause interruption of the electricity supply is insulator failure [21, 35]. This can be caused by problems associated with manufacturing defects, mechanical damage, incorrect installation, electrical tracking, and erosion, among others [21].

Electrical tracking occurs along tracks on the surface of the material, produced by the action of electrical discharges. The surface resistivity of HDPE used in electrical insulators hinders circulation of electric current on the surface, consequently avoiding tracking. However, environmental factors such as contamination of the surface with industrial pollutants, salt, and other substances, with high humidity, act to decrease the surface resistivity and facilitate current flow between different potentials. This current circulating on the surface of the material, due to the conductive film formed by the adhered pollutants, can lead to surface electrical discharges that carbonize the material and initiate track formation [36].

Therefore, in order to avoid tracking, it is important to avoid the adhesion of dirt on the surface of the insulator, which can be assisted by creating a hydrophobic surface. The presence of a hydrophobic or superhydrophobic surface on the insulator confers a self-cleaning characteristic, reducing the accumulation of pollutants, increasing insulator performance, and reducing failures.

Based on this, this work aims to modify the surface of HDPE with TiO₂ nanoparticles in order to obtain materials with these self-cleaning characteristics, which can be applied in polymeric insulators in the distribution network. In order to increase the interaction between the polymer and nanoparticles that have different polarities, it is necessary to functionalize the nanoparticles with specific reagents that interact with both the nanoparticles and the polymer.

In this work, the surface of HDPE was modified by coating with TiO₂ nanoparticles functionalized using four agents to confer hydrophobicity: trimethoxypropylsilane (TMPSi), trimethoxyoctylsilane (TMOSi), trimethoxyhexadecylsilane (TM16Si), and trimethoxyoctadecylsilane (TM18Si). These coatings were applied by immersion processes, both vertically and horizontally, and the evaluation was performed by studying the hydrophobicity of the surfaces using contact angle measurements.

2. MATERIALS AND METHODS

2.1 Materials

High-density polyethylene (type HC 7260 was obtained from Braskem S/A – Brazil). TMPSi, TMOSi, TM16Si, TM18Si, and TiO₂ (rutile) nanoparticles (NPs) smaller than 100 nm were purchased from Sigma-Aldrich. Chloroform, xylene, and isopropyl alcohol (all analytical grade) were obtained from Synth. Heptane (analytical grade) was obtained from Química Moderna. All the reagents were used as received, without further treatment.

2.2 Preparation of the HDPE samples

Samples of HDPE with thickness of 2 mm were produced in the form of plates, by molding using HDPE pellets in a hydraulic thermopress (PHS 15, Schulz) at 165 °C, no load for 4 min, 2 ton for 3 min, 4 ton for 3 min and 6 ton for 1 min. The samples were cooled to ambient temperature for 24 h, cut to sizes of 2.0 x 4.5 cm, and cleaned sequentially using heptane, chloroform, and isopropanol (in this order), in an ultrasonic bath

for 10 min for each solvent. The samples were then allowed to dry for 24 h at ambient temperature. All the HDPE samples used in the work were submitted to the cleaning procedure.

2.3 Functionalization of the NPs and deposition on the HDPE samples

Preparation of the functionalized TiO₂ NPs was performed using 30 mL volumes of solutions of xylene/TMXSi (95/5% v/v), where X represents the functionalization agents with different carbon chain configurations. The solutions were stirred for 5 min, followed by addition of 0.15 g of the TiO₂ NPs (0.5% w/v). The mixtures were ultrasonicated (Ultronic sonicator) for 3 h at ambient temperature.

In the next step, the functionalized nanoparticles were heated to 100 °C, prior to immersion of the HDPE samples for 15 s.

The tests were performed using four functionalization agents with different carbon chain sizes, in order to evaluate their interactions with the polymer surface and obtain maximum adhesion of the nanoparticles to the surface. The molecular structures of the agents (TMPSi, TMOSi, TM16Si, and TM18Si) are shown in Figure 1.

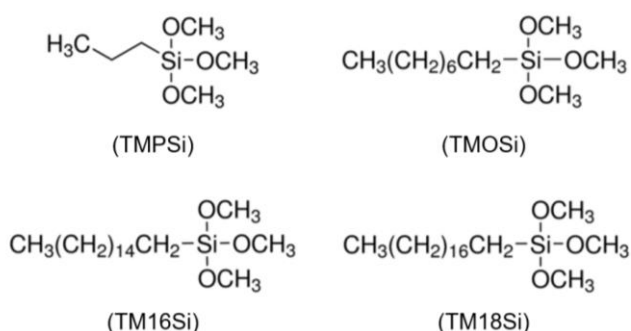


Figure 1. Molecular structures of trimethoxypropylsilane (TMPSi), trimethoxyoctylsilane (TMOSi), trimethoxyhexadecylsilane (TM16Si), and trimethoxyoctadecylsilane (TM18Si) [37-40].

2.3.1 Type of immersion

The samples were immersed in the solutions of functionalized nanoparticles (TiO₂/TMXSi) for 15 s, using a dip-coating process, with the samples in vertical or horizontal positions (Figure 2). The prefix V (vertical) or H (horizontal) indicates the type of immersion. Three samples of each were produced.

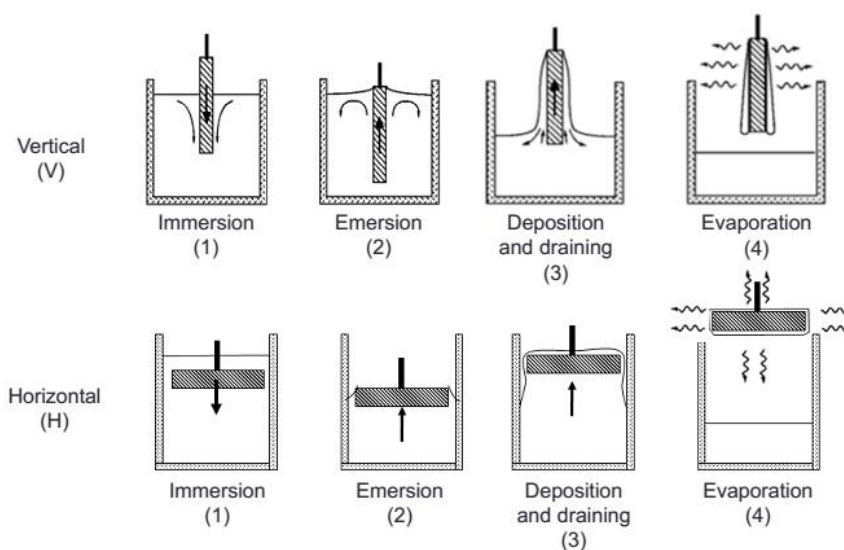


Figure 2. Schematic representation of the dip-coating process.

For comparison, samples were also prepared immersed in the solution with TiO₂ nanoparticles without functionalization, by vertical immersion, called V-HDPE-TiO₂.

2.4 Characterization of the nanoparticles

2.4.1 Band gap determination

Analyses were performed using a UV-Vis spectrophotometer (UV-2401, Shimadzu) to determine the band gap value of the TiO₂ nanoparticles (rutile phase, <100 nm). The spectrophotometer was equipped with a diffuse reflectance accessory, and BaSO₄ was used as a reference

The band gap was calculated according to the methodology for solid particles, by drawing tangents in the spectrum obtained from the reflectance data in the 750-240 nm region, applying the Kubelka-Munk function (as explained below), which resulted in a spectrum equivalent to absorption. The Kubelka-Munk function was used to obtain Tauc plots, with the energy-dependent absorption coefficient (α) calculated using Equation 1 [41]:

$$(\alpha \cdot hv)^{1/\gamma} = B(hv - E_g) \quad (1)$$

where, h is the Planck constant, v is the photon frequency, E_g is the gap energy, and B is a constant. The factor γ depends on the nature of the electron transition (1/2 or 2 for the direct and indirect transition band gaps, respectively, for TiO₂, with indirect type transition normally being considered). The band gap energy is usually determined from diffuse reflectance spectra. According to the theory of Kubelka and Munk (1931), measured reflectance spectra may be transformed into the corresponding absorption spectra by application of the Kubelka-Munk function, shown in Equation 2 [41]:

$$F(R_\infty) = \frac{(1-R_\infty)^2}{2R_\infty} \quad (2)$$

where, R_∞ is the relation between the sample and reference reflectances. Substituting α in Equation 1 for Equation 2 gives Equation 3:

$$(F(R_\infty) \cdot hv)^{1/\gamma} = B(hv - E_g) \quad (3)$$

The analyses were performed for the nanoparticles before and after functionalization, in duplicate.

2.4.2 Determination of crystallite size

The crystallite size (D) was determined by X-ray diffractometry (XRD), employing a diffractometer (D8 ADVANCE ECO, Bruker) containing a copper target X-ray tube, with Cu K α = 0.154060 nm. The instrument was operated at a current of 25 mA, voltage of 40 kV, step of 0.02 s, step time of 0.4 s, and scanning between 2θ of 15° and 80°. The ratio between the rutile and anatase phases was calculated using the software of the equipment, Diffrac.Suite EVA, version 4.2.2.3.

The calculation of D considered the highest intensity TiO₂ diffraction peak, applying the Scherrer equation, where K is a constant (0.89), λ is the X-ray wavelength (Cu K α = 0.15406 nm), β is the width at half height, and θ is the diffraction angle.

2.5 Evaluation of nanoparticle functionalization

The functionalization of the nanoparticles was evaluated using Fourier transform infrared (FTIR) spectroscopy. The NPs functionalized with TMPSi were filtered under vacuum, using an alumina membrane with porosity of 0.02 μ m (Sigma-Aldrich), washed with xylene, and dried for 24 h at 80 °C in an oven.

After drying, the NPs were analyzed using an infrared spectrometer (Tensor 27, Bruker), with scanning from 4000 to 600 cm⁻¹, at resolution of 4 cm⁻¹, and accumulating 32 scans per spectrum, using KBr inserts.

2.6 Evaluation of hydrophobicity of HPDE and adhesion of nanoparticles

After deposition of the functionalized NPs on the HDPE, the hydrophobicity of the samples was determined by the contact angle method, involving measurement of the angle formed between a drop of water and the sample surface. A larger angle indicates less interaction of the water with the surface, reflecting greater hydrophobicity [42]. The analyses were performed in triplicate, using a Theta Lite Optical Tensiometer, from

Biolin Scientific, with CMOS 1/2" USB 3.0 digital camera with fixed zoom and a 10 μ L micropipette, during 30 s of contact of the drop with the surface.

A surface is considered superhydrophilic when the contact angle is approximately 0° ($\theta \approx 0^\circ$), hydrophilic when ($\theta < 30^\circ$), intermediate ($30^\circ < \theta < 90^\circ$), hydrophobic ($90^\circ < \theta < 150^\circ$) and superhydrophobic ($\theta > 150^\circ$) according to the contact angle measurements [43].

2.6.1 Test with water

Qualitative evaluation of adherence of the functionalized nanoparticles on the surfaces of the HDPE samples was performed using tests with water jets, employing a wash bottle. Approximately 50-100 mL of distilled water was used, with jets directed at the upper part of the sample positioned at an angle of approximately 45° .

2.6.2 Tests after physical contact

Qualitative adherence of the nanoparticles was also evaluated after physical contact between paper and the surfaces of the treated HDPE samples. The surfaces were each "cleaned" twice in this way. These tests were performed after the water jet tests, using the same specimens.

3. RESULTS AND DISCUSSION

3.1 Characterization of the nanoparticles

3.1.1 Determination of the band gap value

Figure 3 shows the curves obtained from the diffuse reflectance data for the solid samples, required for calculation of the band gap. The analyses were performed after functionalization of the TiO₂-rutile NPs, using the different functionalization agents, followed by filtration. The results are shown in Table 1.

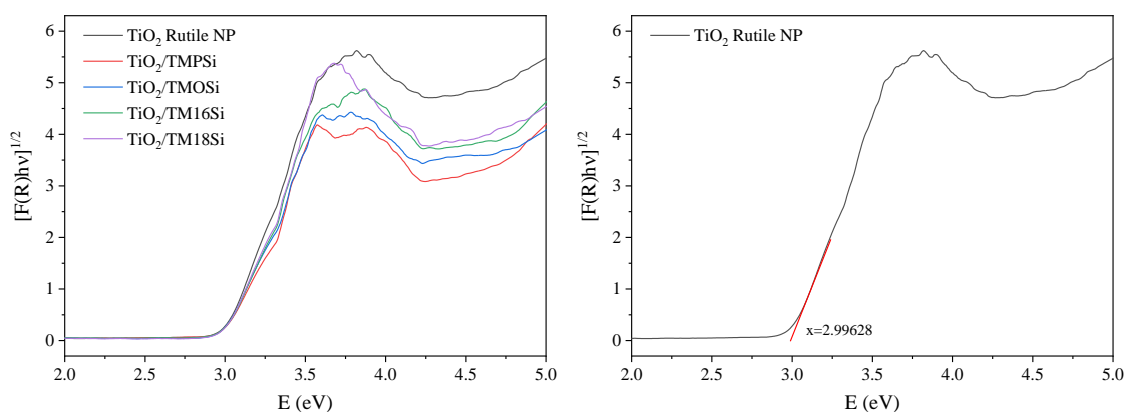


Figure 3. Tauc plots of the spectra: A) TiO₂ nanoparticles before and after functionalization; B) Example of determination of the band gap energy.

Table 1. Band gaps of the functionalized rutile TiO₂ nanoparticles.

SAMPLE	BAND GAP (eV)
TiO ₂ Rutile NP	3.0008 ± 0.0004
TiO ₂ /TMPSi	2.9978 ± 0.0043
TiO ₂ /TMOSi	2.9991 ± 0.0042
TiO ₂ /TM16Si	3.0001 ± 0.0007
TiO ₂ /TM18Si	3.0025 ± 0.0008

The values obtained for the rutile nanoparticles were similar to those reported in the literature for rutile (between 2.97 and 3.08 eV) [8-10, 44, 45]. It should be noted that the band gap value is influenced by the crystalline structure, the crystallite size, and the proportion between the phases [3, 46].

The results showed that the values were not significantly different after functionalization. The band

gap is related to the interaction of the nanoparticle with radiation. After functionalization, the molecules were attached to the surfaces of the nanoparticles by means of interactions involving the active sites with hydroxyls. Since rutile has few of these sites, the functionalization did not alter the crystalline structure or the crystallite size, so it did not affect the band gap value.

3.1.2 Determination of crystallite size

Diffractograms for the nanoparticles before and after functionalization are shown in Figure 4, together with the corresponding Miller indices [8, 47, 48]. The functionalized nanoparticles were filtered prior to the analysis. The calculated crystallite sizes are shown in Table 2.

As in the case of the band gap, functionalization did not lead to any alteration of the sample diffractograms, since it did not change the crystallinity of the nanoparticles.

The calculated crystallite sizes were between 60 and 70 nm. This variation between the samples was anticipated, since the purchased nanoparticles were stated to be smaller than 100 nm, due to the wide size distribution of the powders.

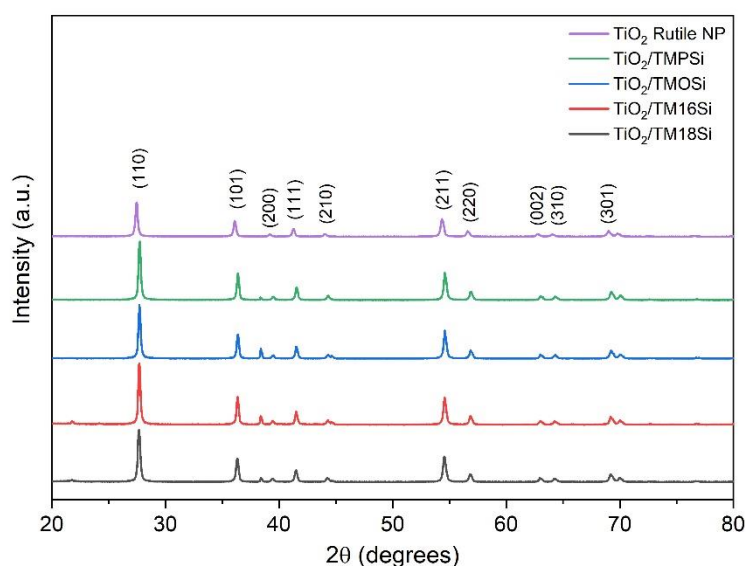


Figure 4. XRD patterns of the rutile TiO_2 nanoparticles before and after functionalization with TMPSi, TMOSi, TM16Si, or TM18Si.

Table 2. Crystallite sizes of the TiO_2 samples with and without functionalization.

SAMPLE	CRYSTALLITE SIZE (nm)
TiO_2 rutile NP	63.9
$\text{TiO}_2/\text{TMPSi}$	72.2
$\text{TiO}_2/\text{TMOSi}$	71.7
$\text{TiO}_2/\text{TM16Si}$	71.9
$\text{TiO}_2/\text{TM18Si}$	62.6

Calculation of the phases present in the samples, using the instrument software, indicated that they were composed of 100% rutile phase. According to the literature, residual amounts of other phases are always present [3]. However, since the quantities are very small (ppm), the equipment was insufficiently sensitive to detect them.

3.2 Assessment of nanoparticle functionalization

FTIR analysis of the nanoparticles was performed before and after functionalization with trimethoxypropylsilane (TMPSi). In order to improve the reliability of the results, after analysis of the

functionalized nanoparticles, they were washed again with xylene, dried, and analyzed a second time. The results are shown in Figure 5.

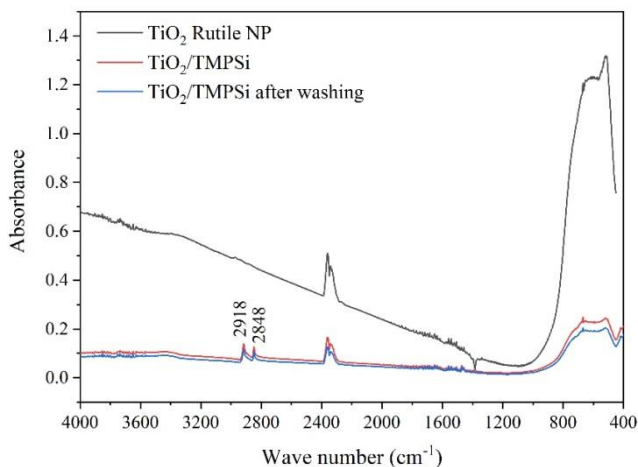


Figure 5. FTIR spectra of the samples.

The spectra of the functionalized nanoparticles showed two absorption bands, at 2918 and 2848 cm^{-1} , corresponding to asymmetric and symmetric stretching, respectively, of the C-H bonds characteristic of the carbon chain of the propyl radical of the functionalization agent [49]. This confirmed that functionalization had occurred, since these bands remained present in the spectra of the materials, even after washing with solvent.

3.3 Hydrophobicity assessment

Qualitative assessment of adhesion of the nanoparticles deposited on the HDPE surface was performed considering the change in hydrophobicity after the test with the water jet and physical contact. In this indirect method, maintenance of hydrophobicity after the tests would indicate continued adhesion of the nanoparticles on the HDPE surface, while decreased hydrophobicity would indicate lower adhesion and removal of the nanoparticles during the tests.

The results are shown in Table 3 and Figure 6 (including the contact angles obtained for the HDPE before and after the washing step that preceded the immersions).

Table 3. Contact angle results for the samples before and after functionalizations with TMOSi, TMPSi, TM16Si, and TM18Si, under the same conditions.

SAMPLE	INITIAL CONTACT ANGLE (°)	CONTACT ANGLE AFTER WATER JET (°)	CONTACT ANGLE AFTER WATER JET AND PHYSICAL CONTACT (°)
V-HDPE-TiO ₂	123.2 ± 11.2	97.5 ± 3.2	-
H-TiO ₂ .TMOSi	138.1 ± 2.2	133.9 ± 16.9	135.8 ± 9.7
V-TiO ₂ .TMOSi	118.2 ± 2.3	117.0 ± 5.5	113.8 ± 14.5
H-TiO ₂ .TMPSi	140.8 ± 8.8	136.7 ± 12.9	129.4 ± 12.8
V-TiO ₂ .TMPSi	120.5 ± 9.7	124.8 ± 4.6	116.6 ± 8.4
H-TiO ₂ .TM16Si	129.3 ± 3.0	131.2 ± 1.7	124.5 ± 16
V-TiO ₂ .TM16Si	111.1 ± 3.5	108.5 ± 4.6	104.3 ± 3.8
H-TiO ₂ .TM18Si	129.7 ± 8.8	138.1 ± 7.0	133.9 ± 11.3
V-TiO ₂ .TM18Si	111.2 ± 3.2	114.9 ± 3.3	108.7 ± 5.0

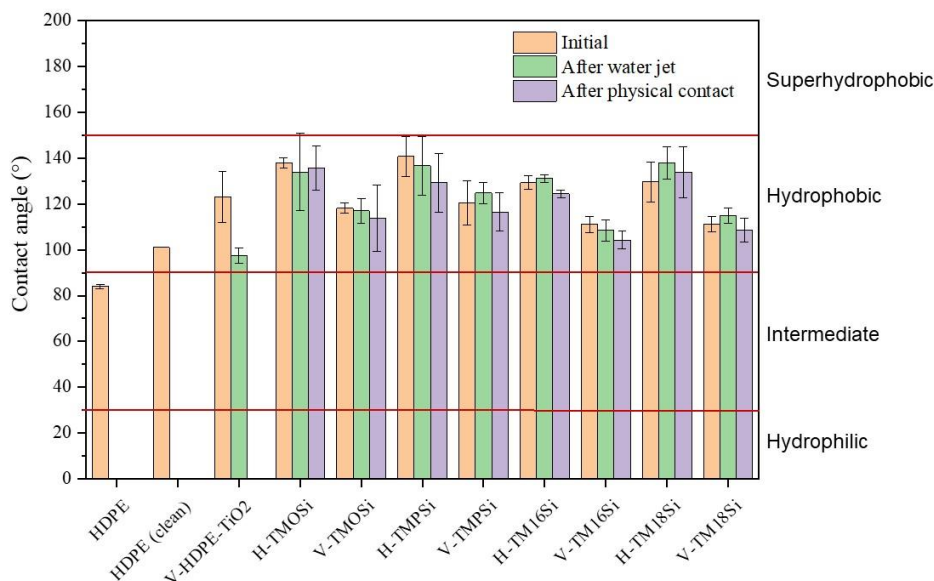


Figure 6. Contact angles for the initial HDPE and the samples produced using different functionalization agents, employing 0.5% of TiO₂ and immersion for 15 s. The prefixes “H” and “V” indicate horizontal and vertical immersion, respectively.

The highest initial contact angles were obtained for the samples horizontally immersed in the solutions containing TiO₂ functionalized with TMPSi (140.8 ± 8.8)° and TMOSi (138.1 ± 2.2)°. However, the lowest variability of the results and the smallest change after the test using the water jet and physical contact were obtained for the sample horizontally immersed in the solution containing TiO₂ functionalized with TM16Si, for which the initial value was (129.3 ± 3.0)° and the value after the tests was (124.5 ± 1.6)°.

All the samples produced by immersion showed increased hydrophobicity, however, when qualitatively evaluating the adhesion of nanoparticles to the polymer surface, it is observed that in the V-HDPE-TiO₂ sample after water jet, the nanoparticles were removed, while the samples produced with functionalized nanoparticles, both horizontally and in the vertical with the 4 agents, this removal of nanoparticles was not observed.

4. CONCLUSIONS

The successful functionalization of the TiO₂ nanoparticles with trimethoxypropylsilane (TMPSi), using the method developed in this work, was confirmed by analysis using FTIR.

Determination of the band gap values of the nanoparticles before and after functionalization showed that the polymeric chains anchored on the surfaces had no effect on the photocatalytic properties.

The dip-coating immersion process, whether performed horizontally or vertically, effectively increased the hydrophobicity of the sample surface. The functionalized HDPE samples produced using TMPSi qualitatively presented the greatest adhesion of the nanoparticles, as shown by comparing the initial contact angle with the values obtained after the water jet and physical contact assays. The highest contact angles were obtained for the samples produced with TMPSi and TMOSi.

The four chemical agents studied here provided functionalization of the nanoparticle surfaces. After preparation of the solutions and immersion of the HDPE, the resulting samples presented surfaces with increased hydrophobicity and qualitative adhesion of the nanoparticles.

In future work, quantification will be made of adhesion of the nanoparticles on the functionalized HDPE surfaces, comparing the initial values with the those obtained after submitting the materials to assays with the water jet and physical contact, as well as after periods of exposure to artificial weathering.

5. ACKNOWLEDGMENTS

The authors thank COPEL DIS and Lactec for financial and technical support of this research. This paper constitutes part of the R&D program of ANEEL (Intelligent Insulator - New mechanisms for surface protection and improvement of the properties of materials – PD 02866-0376/2013).

6. REFERENCES

- [1] COUTINHO, F.M.B., MELLO, I.L., MARIA, L.C.D.S. Polietileno: principais tipos, propriedades e aplicações. *Polímeros: Ciência e Tecnologia*, v. 13, p. 1-13, 2003.
- [2] WEARN, Y.N., MONTAGNA, L.S., PASSADOR, F.R. Compósitos de fibra de coco/LDPE: efeito do tratamento superficial das fibras de coco em compósitos verdes. *Revista Matéria*, v. 25, n. 1, 2020.
- [3] HANAOR, D.A.H., SORRELL, C.C. Review of the anatase to rutile phase transformation. *Journal of Materials Science*, v. 46, p. 855-874, February 2011.
- [4] SALEIRO, G.T., *et al.* Avaliação das fases cristalinas de dióxido de titânio suportado em cerâmica vermelha. *Cerâmica*, v. 56, p. 162-167, 2010.
- [5] SHAMSUDIN, S., *et al.* Hydrophobic rutile phase TiO₂ nanostructure and its properties for self-cleaning application. *AIP Conference Proceedings*. [S.l.]: [s.n.]. 2017. p. 10.
- [6] ZHOU, X., *et al.* Fabrication of superhydrophobic TiO₂ quadrangular nanorod film with self-cleaning, anti-icing properties. *Ceramics International*, v. 45, p. 11508-11516, 2019.
- [7] TAVARES, M.T.S., *et al.* TiO₂/PDMS nanocomposites for use on self-cleaning surfaces. *Surface & Coatings Technology*, v. 239, p. 16-19, 2014.
- [8] CHOUDHURY, B., CHOUDHURY, A. Oxygen defect dependent variation of band gap, Urbach energy and luminescence property of anatase, anatase-rutile mixed phase and of rutile phases of TiO₂ nanoparticles. *Physica E*, v. 56, p. 364-371, 2014.
- [9] MO, L.-B., *et al.* Band gap engineering of TiO₂ through hydrogenation. *Applied Physics Letters*, v. 105, 2014.
- [10] DUBEY, R.S., PRADEEP, D. Experimental study of rutile crystalline phase titania nanoparticles via chemical route. *Materials Today: Proceedings*, v. 18, p. 402-405, 2019.
- [11] HUANG, Z., *et al.* Environmentally durable superhydrophobic surfaces with robust photocatalytic self-cleaning and self-healing properties prepared via versatile film deposition methods. *Journal of Colloid and Interface Science*, v. 527, p. 107-116, 2018.
- [12] QING, Y., *et al.* Facile fabrication of superhydrophobic surfaces with corrosion resistance by nanocomposite coating of TiO₂ and polydimethylsiloxane. *Colloids and Surfaces A: Physicochemical and Engineering Aspects*, v. 484, p. 471-477, 2015.
- [13] ZHANG, X., *et al.* Self-cleaning superhydrophobic surface based on titanium dioxide nanowires combined with polydimethylsiloxane. *Applied Surface Science*, v. 284, p. 319-323, 2013.
- [14] OU, X., LIN, Z., LI, J. Surface microstructure engenders unusual hydrophobicity in phyllosilicates. *Chemical Communications*, v. 54, p. 5418-5421, 2018.
- [15] LIU, P., *et al.* Improving water-injection performance of quartz sand proppant by surface modification with surface-modified nanosilica. *Colloids and Surfaces A: Physicochemical and Engineering Aspects*, v. 470, p. 114-119, 2015.
- [16] ACAR, I., ACISLI, O. Mechano-chemical surface modification of calcite by wet-stirred ball milling. *Applied Surface Science*, v. 457, p. 208-2013, november 2018.
- [17] EYKENS, L., *et al.* Atmospheric plasma coatings for membrane distillation. *Journal of Membrane Science*, v. 554, p. 175-183, may 2018.
- [18] AWAJA, F., *et al.* Adhesion of polymers. *Progress in Polymer Science*, p. 948-968, 2009.
- [19] CHAGAS, G.R., WEIBEL, D.E. Development of poly(propylene) superhydrophobic surfaces by functionalised TiO₂ nanoparticles: effect of solvents and dipping times. *Macromolecular Symposia*, v. 344, p. 55-62, october 2014.
- [20] ABRADÉE - ASSOCIAÇÃO BRASILEIRA DE DISTRIBUIDORES DE ENERGIA ELÉTRICA. A Distribuição de energia, 2018. Disponível em: <<https://www.abradee.org.br/setor-de-distribuicao/a-distribuicao-de-energia/>>. Acesso em: 28 novembro 2020.
- [21] MARTINS, R., SWINKA, V. Development of a thermochromic polymer insulator. *IEEE Latin America Transactions*, v. 16, p. 813-818, 2018.
- [22] SILVA, A.A.P., *et al.* Linha de distribuição experimental para desenvolvimento de técnica de monitoração de isoladores poliméricos. *Simpósio Brasileiro de Sistemas Elétricos (SBSE)*. Goiânia: [s.n.]. 2012. p. 5.
- [23] ABNT. ABNT NBR 16327-1:2014 - Isolador polimérico tipo pino para redes com cabos cobertos fixados em espaçadores, para tensões acima de 1000 V - Parte 1: Definição, métodos de ensaio e critérios de aceitação. Associação Brasileira de Normas Técnicas (ABNT). [S.l.], p. 23. 2014.
- [24] ANBT. ABNT NBR 16327-2:2014 - Isolador polimérico tipo pino para redes com cabos cobertos fixados em

- espaçadores, para tensões acima de 1000 V - Parte 2: Dimensões e características. Associação Brasileira de Normas Técnicas (ABNT). [S.l.], p. 23. 2014.
- [25] ABNT. ABNT NBR 16094:2017 - Acessórios poliméricos para redes aéreas de distribuição de energia elétrica - Requisitos de desempenho e métodos de ensaio. Associação Brasileira de Normas Técnicas (ABNT). [S.l.], p. 34. 2017.
- [26] ABNT. ABNT NBR 16095:2017 - Acessórios poliméricos para redes aéreas de distribuição de energia elétrica - Requisitos construtivos. Associação Brasileira de Normas Técnicas (ABNT). [S.l.], p. 18. 2017.
- [27] SAMPERS, J. Importance of weathering factors other than UV radiation and temperature in outdoor exposure. *Polymer Degradation and Stability*, v. 76, p. 455-465, 2002. Disponível em: <[https://doi.org/10.1016/S0141-3910\(02\)00049-6](https://doi.org/10.1016/S0141-3910(02)00049-6)>.
- [28] DEHBI, A., *et al.* Degradation of thermomechanical performance and lifetime estimation of multilayer greenhouse polyethylene films under simulated climatic conditions. *Polymer Engineering and Science*, v. 55, p. 287-298, 2015. Disponível em: <<https://doi-org.ez22.periodicos.capes.gov.br/10.1002/pen.23895>>.
- [29] MARIA, R., *et al.* Monitoring the influence of different weathering conditions on polyethylene pipes by IR-microscopy. *Polymer Degradation and Stability*, v. 96, p. 1901-1910, 2011.
- [30] FERLUGA, A., CANIATO, M., SBAIZERO, O. The influence of consolidation and artificial weathering on all-PP composite behavior. *Journal of Applied Polymere Science*, v. 132, p. 41283-, 2015.
- [31] GIJSMAN, P., HENSEN, G., MAK, M. Thermal initiation of the oxidation of thermoplastic polymers (Polyamides, Polyesters and UHMwPE). *Polymer Degradation and Stability*, v. 183, p. 109452, January 2021.
- [32] CHIRINOS-PADRÓN, A.J., *et al.* Influences of unsaturation and metal impurities on the oxidative degradation of high density polyethylene. *European Polymer Journal*, v. 23, p. 935-940, 1987.
- [33] JIN, C., *et al.* Effect of anisotropy on photo-mechanical oxidation of polyethylene. *Polymer*, v. 44, p. 5969-5981, 2003.
- [34] YEH, C.-L., *et al.* The effect of common agrichemicals on the environmental stability of polyethylene films. *Polymer Degradation and Stability*, v. 120, p. 53-60, 2015.
- [35] THOMAZINI, D. Classificação da hidrofobicidade em isoladores elétricos poliméricos de alta tensão. Universidade de São Paulo. [S.l.], p. 149. 2009.
- [36] MUNARO, M., *et al.* Fatores de influência na compatibilidade de cabos protegidos, isoladores e acessórios utilizados em redes aéreas compactas de distribuição de energia elétrica, sob condições de multi-estressamento. II Congresso de Inovação Tecnológica em Energia Elétrica. [S.l.]: [s.n.]. 2003. p. 555-560.
- [37] KGAA, M. Trimethoxy(propyl)silane Sigma-Aldrich. Site da Merck. Disponível em: <<https://www.sigmaaldrich.com/catalog/product/aldrich/662275?lang=pt®ion=BR>>. Acesso em: 24 mar. 2019.
- [38] KGAA, M. Trimethoxy(octyl)silane Sigma-Aldrich. Site da Merck. Disponível em: <<https://www.sigmaaldrich.com/catalog/product/aldrich/376221?lang=pt®ion=BR>>. Acesso em: 15 abr. 2020.
- [39] KGAA, M. Hexadecyltrimethoxysilane Sigma-Aldrich. Site da Merck. Disponível em: <<https://www.sigmaaldrich.com/catalog/product/aldrich/52360?lang=pt®ion=BR>>. Acesso em: 17 fev. 2020.
- [40] KGAA, M. Trimethoxy(octadecyl)silane. Site da Merck. Disponível em: <https://www.sigmaaldrich.com/catalog/product/aldrich/376213?lang=pt®ion=BR&cm_sp=Insite-_-caContent_prodMerch_cooccuranceModel-_prodMerch10-4>. Acesso em: 17 fev. 2020.
- [41] MAKUŁA, P., PACIA, M., MACYK, W. How To Correctly Determine the Band Gap Energy of Modified Semiconductor Photocatalysts Based on UV-Vis Spectra. *Journal of Physical Chemistry Letters*, v. 9, p. 6814-6817, 2018.
- [42] ABNT. ABNT IEC/TS 62073 - Orientações para medição da hidrofobicidade na superfície de isoladores. Associação Brasileira de Normas Técnicas (ABNT). [S.l.]. 2018.
- [43] MUNARO, A.P. Processos de degradação de borrachas de polidimetilsiloxano: mecanismos e avaliação de propriedades. Universidade Federal do Paraná (UFPR). Curitiba, p. 64. 2018.
- [44] GUPTA, S.M., TRIPATHI, M.A review of TiO₂ nanoparticles. *Chinese Science Bulletin*, Junho 2011. 1639-1657.
- [45] WANG, Y., *et al.* Engineering the band gap of bare titanium dioxide materials for visible-light activity: A theoretical prediction. *RSC Advances*, v. 3, p. 8777-8782, 2013.
- [46] FELTRIN, J., *et al.* Superfícies fotocatalíticas de titânia em substratos cerâmicos. Parte I: Síntese, estrutura e fotoatividade. *Cerâmica*, 2013. 620-632.
- [47] SCARPELLI, F., *et al.* Mesoporous TiO₂ Thin Films: State of the Art. In: _____ Titanium Dioxide - Material for a Sustainable Environment. [S.l.]: Intech Open, 2018. Cap. 3, p. 57-80.
- [48] MERIN, K.T., *et al.* Effect of Zinc concentration in TiO₂ nanoparticles synthesized by Sol-Gel technique for Photocatalytic Applications. *Materials Today: Proceedings*, v. 33, p. 2315-2320, 2020.
- [49] SILVERSTEIN, R.M., WEBSTER, F.X., KIEMLE, D.J. Identificação Espectrométrica de Compostos Orgânicos. [S.l.]: LTC, 1963.

ORCID

Aline Souza Salum

<https://orcid.org/0000-0001-5781-7765>

Paulo Apolinário da Silva Veiga

<https://orcid.org/0000-0001-7354-0778>

Joseane Valente Gulmine

<https://orcid.org/0000-0002-3675-9102>

Vitoldo Swinka Filho

<https://orcid.org/0000-0003-4622-909X>